metals

MDPI

Article

Relationship between Structure and Properties of Intermetallic Materials Based on γ-TiAl Hardened In Situ with Ti_3Al

Varvara Avdeeva [1,*], Arina Bazhina [2], Mikhail Antipov [2], Alexander Stolin [2] and Pavel Bazhin [2]

[1] Kurnakov Institute of General and Inorganic Chemistry, Russian Academy of Sciences, Leninskii Prospekt 31, 119991 Moscow, Russia

[2] Merzhanov Institute of Structural Macrokinetics and Materials Sciences, Russian Academy of Sciences, Akademika Osipyana 8, Chernogolovka, 142432 Moscow, Russia; arina@ism.ac.ru (A.B.); mora1997@mail.ru (M.A.); amstolin@ism.ac.ru (A.S.); bazhin@ism.ac.ru (P.B.)

* Correspondence: avdeeva.varvara@mail.ru

Abstract: In this work, intermetallic materials based on γ-TiAl in situ strengthened with the Ti_3Al phase have been obtained from the initial components of titanium and aluminum under the conditions of free SHS-compression in one technological step and in ten seconds. This method combines the process of the combustion of initial components in the mode of self-propagating high-temperature synthesis (SHS) with high-temperature shear deformation of the synthesized materials. The following initial compositions have been studied (mol): Ti–Al, 1.5 Ti–Al, and 3 Ti–Al. Thermodynamic calculations have been carried out and the actual combustion temperature of the compositions under study has been measured. To increase the exothermicity of the studied compositions, a "chemical furnace" based on a mixture of Ti–C powders has been used, which allows us to increase the combustion temperature and stabilize the combustion front. It has been found that the actual combustion temperature of the selected compositions increased from 890–1120 to 1000–1350 °C. The results of X-ray powder diffraction and SEM are presented, mechanical and tribological characteristics of the obtained materials are measured, and 3D images of wear grooves are given. It has been found that a decrease in Ti molar fraction and an increase in Al molar fraction in the initial mixture lead to an increase in the mechanical (hardness up to 10.2 GPa, modulus of elasticity up to 215 GPa) and tribological characteristics (wear up to 4.5 times, coefficient of friction up to 2.4 times) of intermetallic materials.

Keywords: intermetallic; shear deformation; high temperature; tribology

check for updates

Citation: Avdeeva, V.; Bazhina, A.; Antipov, M.; Stolin, A.; Bazhin, P. Relationship between Structure and Properties of Intermetallic Materials Based on γ-TiAl Hardened In Situ with Ti_3Al. *Metals* **2023**, *13*, 1002. https://doi.org/10.3390/met13061002

Academic Editors: Jayalakshmi Subramanian and Chonghe Li

Received: 26 April 2023
Revised: 17 May 2023
Accepted: 19 May 2023
Published: 23 May 2023

Copyright: © 2023 by the authors. Licensee MDPI, Basel, Switzerland. This article is an open access article distributed under the terms and conditions of the Creative Commons Attribution (CC BY) license (https://creativecommons.org/licenses/by/4.0/).

1. Introduction

At present, intermetallic materials and alloys based on γ-TiAl are attracting increased attention as high-temperature structural materials due to their light weight, high specific modulus of elasticity, high specific strength, and heat resistance [1–3]. The manufacture of finished products from intermetallic materials is a promising direction in the aerospace and automotive industries for turbine blades, bearings, and exhaust valves [4–6]. The replacement of currently existing nickel-based superalloys [7–9] with alloys based on titanium aluminides will make it possible to reduce the weight of gas turbine engine parts by up to 1.5–2 times (density of nickel superalloys is about 9 g/cm^3, whereas that for alloys based on γ-TiAl is about 4 g/cm^3). In addition, this will also reduce the cost of their manufacture by up to 30%. It is also worth considering, for alloys based on γ-TiAl, an increase in the yield strength with increasing temperature, a high strength/density ratio, resistance to oxidation and ignition, and heat resistance [10–12].

However, to use these intermetallic compounds as new structural materials for the manufacture of turbine blades, turbocharger wheels, exhaust valves, and expanding dampers, both high mechanical properties and high wear resistance are required [13–15]. The scope of intermetallic compounds based on γ-TiAl in a wider range of industrial applications is limited due to their low tribological characteristics [16]. In addition, the use

of alloys based on γ-TiAl is limited due to their insufficient resistance to oxidation at temperatures above 700–750 °C [17,18]. Poor sliding friction and low wear resistance become an obstacle to improving the axial load and service life of γ-TiAl alloy components under extreme conditions [19]. For example, (i) turbine blades have fatigue cracks on their surface because of abrasive wear during operation, which leads to catastrophic consequences; (ii) for automobile exhaust valves, the wear surface is one of the main causes of component failure [20]. Thus, the actual task at present is to improve the frictional and wear-resistant characteristics of intermetallic compounds based on the Ti–Al system. For example, to improve the mechanical and tribological characteristics of the γ-TiAl alloy, it is doped with ceramic particles (Ti_2AlC, Ti_2AlN, SiC, Ti_5Si_3, TiB_2, and Al_2O_3) [21–25], as well as TiC, etc., which are chemically and thermally stable with the TiAl matrix.

Given that intermetallic compounds based on titanium aluminides have low plasticity, especially at low temperatures, many works aim to increase their plasticity. In this case, depending on the grain size and under certain conditions, the TiAl intermetallic compound can exhibit superplasticity. Thus, for a single-phase TiAl intermetallic compound with a fine-grained structure, the relative elongation is 225% at a temperature of 800 °C and a strain rate of 8.3×10^{-4} s^{-1}. To increase the plasticity of titanium aluminide TiAl, researchers alloy them with third components, such as Be, Cr, Nb, Mo, and Ni [26–28]. The creep resistance of intermetallic compounds based on TiAl is increased by alloying with the following chemical elements B, C, Cr, Nb, Ta, W [29,30]. Doping of the TiAl intermetallic compound with elements such as Nb, Si, Ta, and W leads to an increase in heat resistance [31]. The best set of properties is achieved with multicomponent alloying [32].

Promising methods are those related to the in situ hardening of titanium aluminides. Compared to ex situ, these methods are less energy-intensive and more productive. When an additional external load is applied in the process of the in situ hardening of intermetallic materials, compact composites with the desired physical and mechanical characteristics are obtained. In [33], TiAl matrix composites are reinforced with in situ boride precipitation during the isothermal compression. In [34], in situ hardening of the TiAl matrix composite was carried out with the ternary phase of Ti_2AlNb by powder metallurgy methods (hot pressing, hot extrusion, and heat treatment at a temperature of 1280 °C). It was found in the work that the obtained samples have high values of strength and fluidity, as well as high values of impact strength. The explanation for the increase in the mechanical properties of composites based on TiAl is based on the mechanism of dispersion strengthening by the finely dispersed fraction of the Ti_2AlNb phase. Composites based on TiAl are strengthened in situ with intermetallic particles; for example, Ti_5Si_3 [35]. The resulting composites have improved mechanical characteristics, including those observed at high temperatures, compared to cast intermetallic materials based on TiAl. In [36], the deformation behavior of the two-phase nano-polycrystalline alloys TiAl + Ti_3Al was studied. It was established that, at a given temperature, there is a critical grain size, which is the dominant factor that affects the mechanism of deformation of a single-phase TiAl alloy. For two-phase nano-polycrystalline alloys TiAl + Ti_3Al, it was found that, during deformation, the motion of dislocations in TiAl with a grain size less than the critical one predominates, while no such effect was found for the Ti_3Al phase. This work confirms the promise of strengthening the γ-TiAl alloy with the Ti_3Al phase.

In this work, we proposed to obtain, under the conditions of the free SHS-compression method, intermetallic materials based on γ-TiAl in situ strengthened by the Ti_3Al phase when using initial powder titanium and powder aluminum as reagents. This method combines the combustion of the initial components in the self-propagating high-temperature synthesis (SHS) mode with the high-temperature shear deformation of the synthesized materials. The region of homogeneity of the Ti_3Al phase at room temperature is in the range of 15–23 wt % Al and retains its ordered structure up to a temperature of 1090 °C. This phase has a hexagonal close-packed lattice similar to that of the α-phase, but differs from this in the ordered arrangement of titanium and aluminum atoms. In this case, the Ti_3Al phase has a higher hardness (4.54 GPa) than the γ-TiAl phase (3.15 GPa), which allows for

it to be considered as a strengthening phase for the synthesized material. The conditions of the free SHS compression method make it possible to obtain compact materials with a given structure and a given set of physical and mechanical properties from the initial powder components in the combustion mode and high-temperature shear deformation [37–40]. The advantages of this method include the speed of the SHS process (tens of seconds), that there is no need to externally heat the initial components [41–43], the simplicity of the equipment used, and the shear loads used during deformation, which help to reduce the porosity of the material.

The aim of this work is to obtain intermetallic materials based on γ-TiAl that is in situ strengthened by the Ti_3Al phase, using free SHS compression to study the features of their structure, phase composition, mechanical, and tribological properties, as well as to establish their relationship with each other.

2. Materials and Methods

2.1. Objects and Procedures

In this work, we prepared and studied three compositions of the initial mixtures differing in stoichiometry (Table 1). Commercial powder aluminum (<30 μm, 99.7%) and powder titanium (<45 μm, 99.1%) were taken in the molar ratio of Ti–Al, 1.5 Ti–Al and 3 Ti–Al and used as initial components. The initial powders were dried and mixed in predetermined ratios in ball mills with a drum rotation speed of 0.8 rev/s for 12 h (atmospheric pressure, room temperature). The ball-to-powder weight ratio that was missing was 1:3. Next, they were pressed into cylindrical blanks 50 mm in diameter, 30 mm high, with a relative density of 0.8. Since the studied compositions have a weak exothermicity, a "chemical furnace" was prepared to initiate the combustion process in the mode of self-propagating high-temperature synthesis (SHS). This was a cylindrical billet of highly exothermic composition Ti (80 wt %, <45 μm, 99.1%)–C(20 wt %, <1 μm, 99.6%) with a diameter of 50 mm and a height of 5 mm, which was placed on top of a green sample of Ti–Al. The combustion process was initiated with a tungsten coil (voltage 30 V) from the top of the workpiece based on Ti–C (Figure 1). After the combustion wave passed through the green sample and a predetermined time, the synthesized material was compressed by a press plunger at a pressure of 10 MPa. When compressing, the material was deformed at a high temperature at a press-plunger speed of 100 mm/s (in Figure 1, the deformation direction of the synthesized material is indicated by red arrows). After compression, the obtained samples were placed in an oven at T = 500 °C for 2 h and then cooled to relieve thermal stress. After the sample cooled, the upper part, approximately 1 mm high, was mechanically removed. The carbide phase diffusion in intermetallics is no more than 200 μm; therefore, no carbide phase was detected in the studied samples. The height of the resulting sample was controlled by using rigid limiters located along the edges of the platform, based on the fact that the deformed material will not touch these during pressing. In this work, the height of the limiters was 10 mm. As a result, cylindrical compact materials with a diameter of 65 mm and a height of 10 mm were obtained.

2.2. Characterization

To measure the combustion temperature, a tungsten–rhenium thermocouple was placed in the center of each green sample at half the depth of this green sample.

The microstructure of samples was studied on a Carl Zeiss Ultraplus ultra-high-resolution field-emission scanning electron microscope (Carl Zeiss, Neubeuern, Germany). Energy-dispersive analysis was conducted using an INCA 300 X-ray microanalyzer (Oxford Instruments, Great Britain). X-ray powder diffraction studies were performed on an ARL X'TRA diffractometer (Thermo Fisher Scientific, Switzerland). Samples were cut from the plates obtained by erosion. Then, samples were ground and polished by standard methods using diamond pastes of various fineness. SEM and X-ray powder diffraction studies were conducted from the cross-section of samples. X-ray powder diffraction studies were performed using a copper anode.

Table 1. Green sample composition and synthesis parameters.

Composition	Ratio of Initial Components, mol	Composition of Initial Components, wt %		Adiabatic Combustion Temperature (without Chemical Furnace), °C	Combustion Temperature under Experimental Conditions (without Chemical Furnace), °C	Combustion Temperature under Experimental Conditions (with Chemical Furnace), °C	Synthesis Time (with Chemical Furnace), s
		Ti	Al				
I	Ti–Al	64	36	1250	1120	1350	8.5
II	1.5 Ti–Al	72	28	1000	890	1150	10
III	3 Ti–Al	84	16	670	no	1000	16

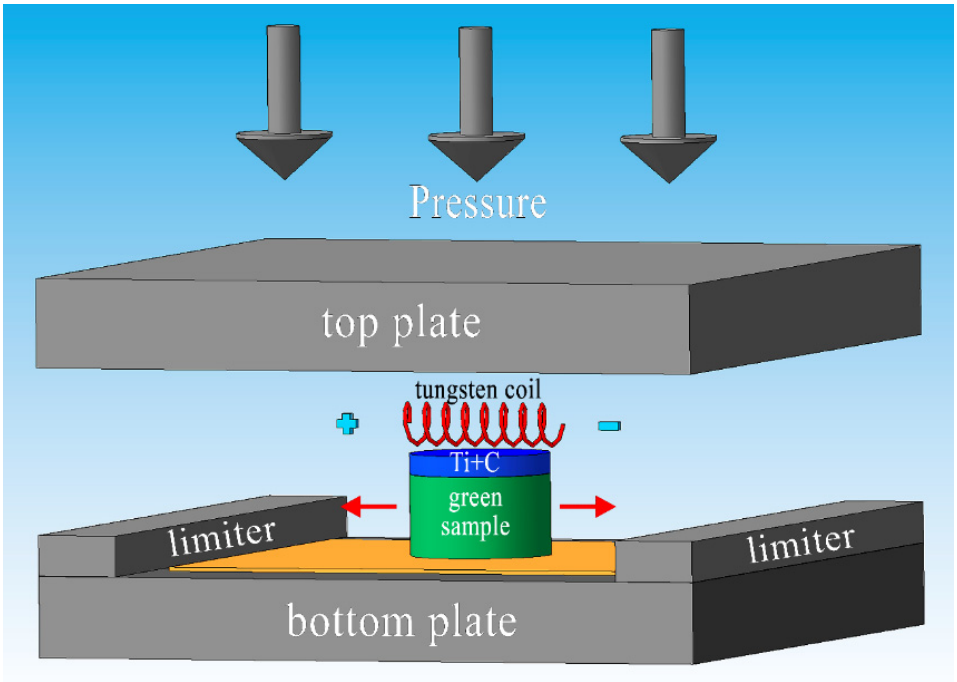


Figure 1. Scheme of the experiment.

2.3. Mechanical Testing

The instrumented indentation was conducted in accordance with ISO 14577–1: 2002 on polished cross-sections of a CSM Nano-Hardness Tester (CSM Instruments, Peseux, Switzerland). All samples were subjected to matrix-instrumented indentation (loading, 10 mN) on a Berkovich-type diamond tip. The measurements were performed in the central part of the section. Maximum loading, 10 mN; loading/unloading rate, 20 mN; contact time, 20 s; distance between prints: x = 15 μm and y = 12 μm. The processing of the experimental curves was realized using the Nanoindentation 3.0 software from CSM Instruments (Switzerland) with the preset Poisson's ratio (0.3) and averaged at one (7–9 experimental curves).

2.4. Tribology Testing

Tribological tests [44] of the samples were carried out on a TRIBOMETER friction machine from CSM Instruments (CSM Instruments, Peseux, Switzerland), using a reciprocating movement according to the "rod-plate" scheme. The parameters are given in Table 2. After testing, the surface of the sample and the counterbody were blown with a jet of dry air to remove wear products and washed in an ultrasonic bath filled with isopropyl alcohol.

Next, 2D profilograms and 3D images of wear grooves on the samples were measured. The counterbody was chosen based on the work [45], in which it was established that the greatest wear of the samples was observed when the Al_2O_3 counterbody was used. Because, in [45] at a load of 10 N, there was too much wear for samples additionally doped with Nb, Cr, and B, in this work, a smaller load of equal to 1 N was chosen. The rest of the parameters were chosen with average values based on a load of 1 N.

Table 2. Technical parameters of tribological tests.

Parameter	Value
Track length	4 mm
Applied load	1 N
Maximum speed	10 cm/s
Counterbody	A ball with a diameter of 3 mm
Counterbody material	Al_2O_3
Run	10,000 cycles (80 m)
Medium	Air

2.5. Thermodynamic Analysis

Thermodynamic calculations were conducted using the ISMAN-Thermo software package. This software is used to calculate thermodynamic equilibria in complex multicomponent heterophase systems and to analyze the possible compositions of inorganic products and the system's adiabatic combustion temperature. The calculation characterizes the equilibrium by minimizing the thermodynamic potential of the system and considers the contributions of thermodynamic potentials of all compounds in the system, as well as their concentrations.

3. Results and Discussion

3.1. Synthesis Characterization

To ensure the flow of synthesis of compositions based on titanium and aluminum in the SHS mode according to the solid-phase mechanism, it is necessary that one of the components melts. Composition I has sufficient exothermicity for successful synthesis in the SHS mode (Table 1). The adiabatic combustion temperature of composition *I* was 1250 °C, and the actual combustion temperature under the experimental conditions with a chemical furnace was 1350 °C. This temperature is enough to melt aluminum and interact with titanium according to the solid-phase mechanism.

When increasing the proportion of titanium in the initial mixture, the exothermicity of the studied compositions sharply decreases. As shown by thermodynamic calculations, the adiabatic combustion temperature decreases by almost two times with an increase in the titanium content and a decrease in aluminum in the initial mixture (Table 1). For composition II, it is possible to initiate a combustion wave in the SHS regime, but an unstable and damped combustion regime is observed. For composition III, it is not possible to initiate a combustion wave in the SHS mode, because the adiabatic combustion temperature is very low (under actual experimental conditions, this is even lower because of the inevitable heat losses) and is at the level of aluminum melting. The thermal impulse created by the tungsten coil under the experimental conditions is not great enough to initiate a chemical reaction between titanium and aluminum.

To increase the exothermicity of the mixture, different approaches are used: preliminary mechanical activation of the initial components [46–48], preliminary heating of the initial green sample [49]. In this work, we used a "chemical furnace", which is a pressed green sample from a mixture of titanium and carbon black. The interaction of titanium with carbon black proceeds by an exothermic mechanism with a thermal effect equal to 3480 kJ/kg and a combustion temperature of more than 3000 °C, which is easily initiated

by a tungsten coil. The use of this "chemical furnace" makes it possible to initiate a combustion wave in all the studied compositions, as well as to increase their actual combustion temperature (Table 1). Let us highlight composition III, in which, using a chemical furnace, we managed to initiate synthesis with a stable combustion wave front in the SHS mode and increase the actual combustion temperature to 1000 °C.

When the combustion wave passed through the green sample and after the specified synthesis time (Table 1), the synthesized material was pressed, creating a sufficient temperature to plastically deform. Intermetallic compounds based on titanium aluminides at temperatures below 700 °C have almost no plasticity, due to the peculiarities of their dislocation structure. The time interval in which the synthesized materials are capable of plastic deformation depends on the combustion temperature of the initial mixture. The higher the combustion temperature of the selected composition, the wider this interval. For the studied intermetallic materials based on Ti–Al under the experimental conditions, this interval is less than a second, which significantly hinders their plastic deformation. Composition *III*, which has the lowest combustion temperature, has the worst plastic deformation. As established earlier [50], the plastic deformation of the studied intermetallic materials occurs due to the motion of dislocations. Increasing the temperature of intermetallic materials, especially above 700 °C, increases their plastic deformation. Thus, even for compositions I and II, an additional increase in the combustion temperature has a positive effect and increases the time interval in which they can plastically deform.

Due to the absence of a side barrier (a characteristic feature of the method of free SHS compression [51–53]), the synthesized material was subjected to both axial and shear deformation (in Figure 1, the direction of deformation of the synthesized material is indicated by red arrows). As a result, due to the additional displacement during the shear deformation of the synthesized material into pores, compact samples with a porosity of less than 2% were obtained.

3.2. X-ray Powder Diffraction and Microstructure

According to the X-ray powder diffraction results (Figure 2), the synthesis and subsequent deformation afforded materials consisting of intermetallic phases γ-TiAl and Ti_3Al (compositions II and III), as well as α-Ti. In addition to these phases, for composition *I*, the $TiAl_3$ phase is observed. Thus, materials based on γ-TiAl in situ hardened with the Ti_3Al phase were obtained from the initial components of titanium, aluminum, and carbon black. A characteristic feature of the obtained materials, as was studied in more detail [54], is the gradient structure of intermetallic phases (Figure 3). This is a consequence of the ongoing thermal diffusion processes during self-propagating high-temperature synthesis and the subsequent sharp decrease in temperature during contact with the press plunger, which completes phase and structure formation. Generally, a hardening of the structure of the material is observed where phase and structure formation are not complete. This is clearly seen for composition *I*, which has the shortest synthesis time because the formation of intermetallic compounds based on Ti–Al occurs due to the melting of aluminum, its spreading through the channels of the capillary–porous medium, and the subsequent diffusion of aluminum atoms into the titanium lattice. This leads to the formation of the primary $TiAl_3$ compound, which subsequently transforms as it is saturated with titanium into TiAl and Ti_3Al. With an increase in the synthesis time, this transformation occurs more completely. Thus, under conditions of free SHS compression, by changing the composition of the green sample and the synthesis time until contact with the press plunger, it is possible to change the phase composition and structure in intermetallic materials. As shown in the study [55], subsequent thermal annealing makes it possible to homogenize the synthesized materials based on Ti–Al.

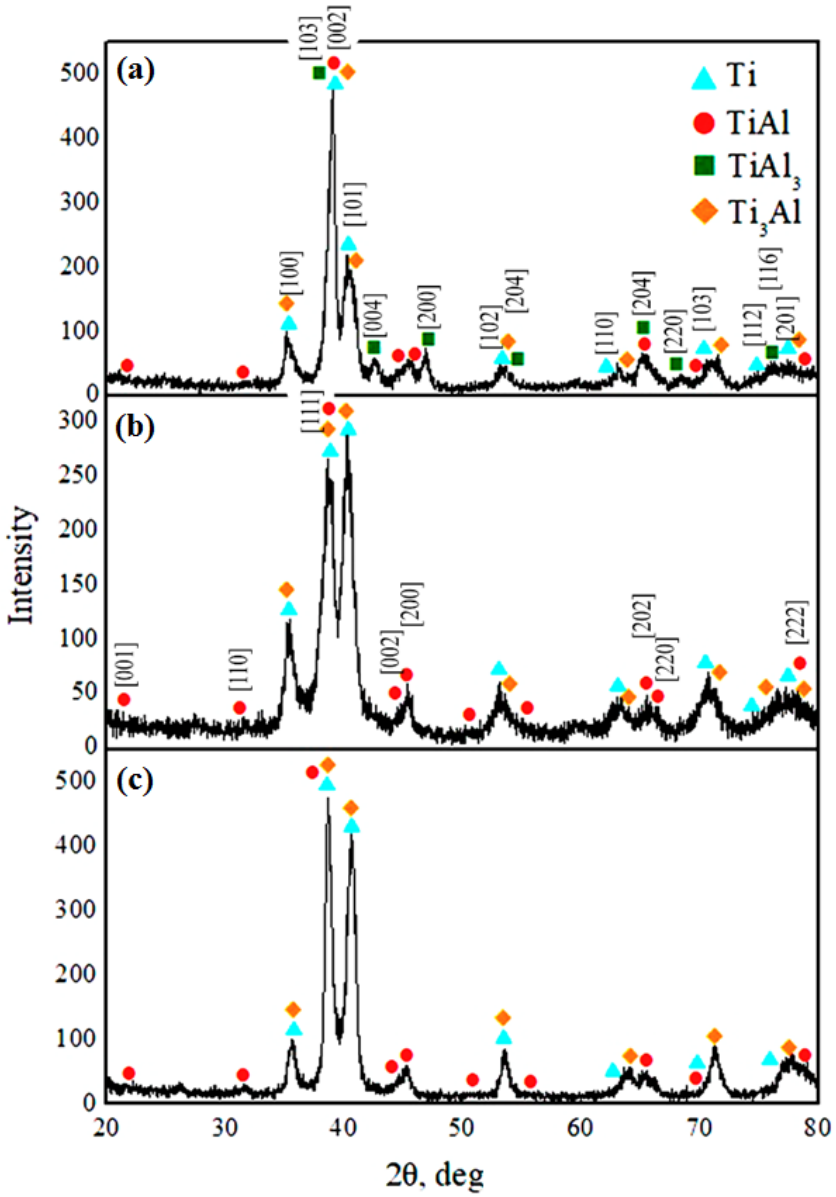


Figure 2. X-ray powder diffraction patterns of compositions: (**a**) I, (**b**) II, and (**c**) III.

It was found [36] that, at temperatures above 527 °C, the deformation mechanism changes in the two-phase nano-polycrystalline alloy TiAl + Ti_3Al. The intermetallic material TiAl + Ti_3Al passes from the mechanism of plastic deformation to the mechanism of boundary slip and recrystallization. Thus, under the experimental conditions in this work, a recrystallized structure is formed in the intermetallic material, represented by the grains of the γ-TiAl phase and precipitates of Ti_3Al. By adjusting the technological parameters of free SHS compression (especially the time from the beginning of the initiation of the combustion process to the application of pressure), as well as the initial composition of intermetallic materials, it is possible to change the grain size of the γ-TiAl phase over a wide range, as well as the size, shape and proportion of the α_2-phase Ti_3Al, and the type of grain boundaries. This structure provides a higher set of mechanical properties at room temperature compared to the lamellar structure [36]. In addition, the structure of intermetallic materials is significantly affected by their degree of deformation. As the degree of deformation increases, the grain size of the material decreases. By changing the height of the limiters in the experiment, we can control the degree of deformation of the synthesized material.

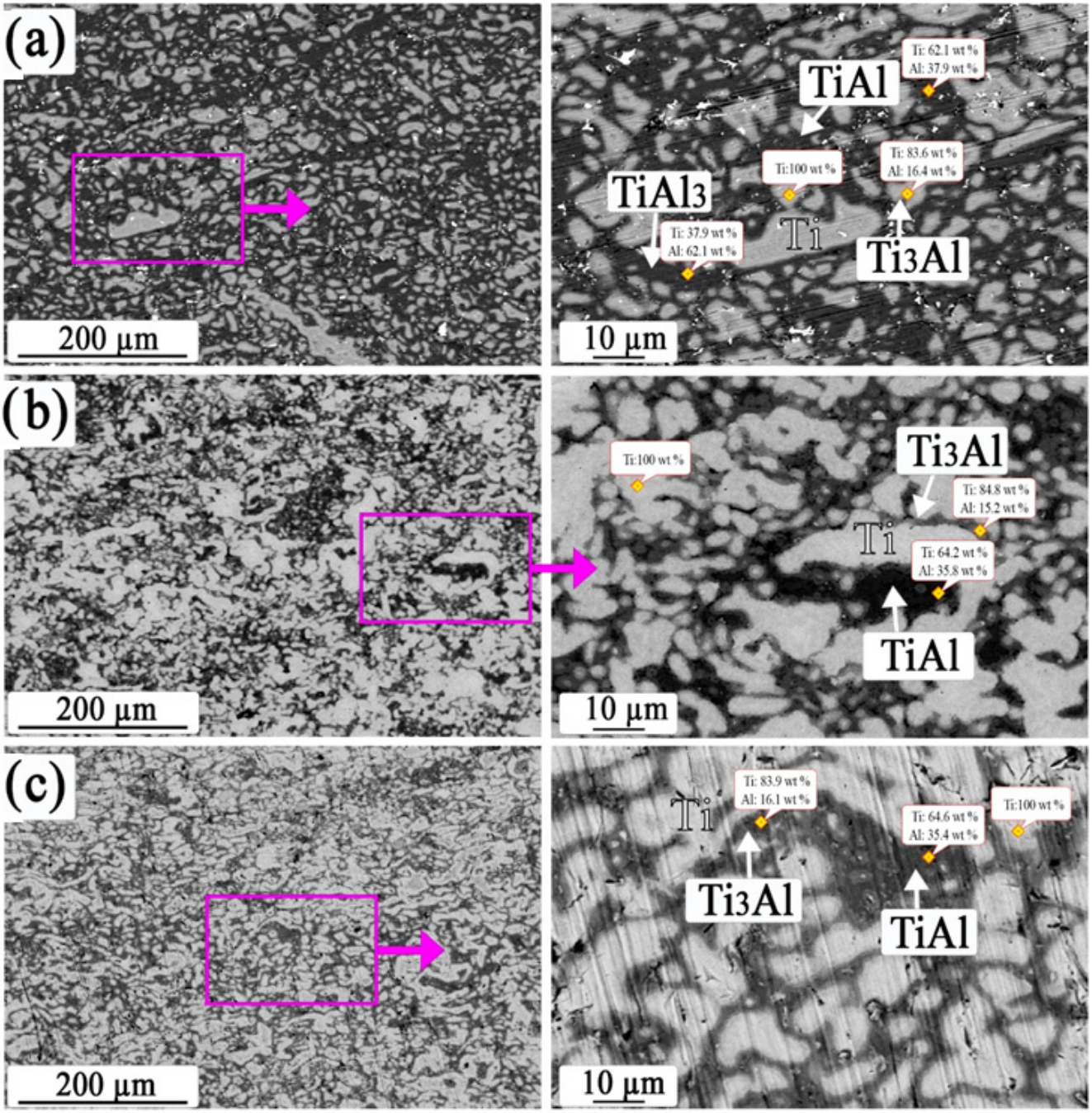


Figure 3. SEM of synthesized materials for compositions: (**a**) I, (**b**) II, and (**c**) III.

3.3. Mechanical Characteristics

As the measurements of the mechanical characteristics of the obtained materials show, the material of composition I has the highest values (Table 3). An increase in the molar content of titanium in the material leads to a decrease in the intermetallic phases, which reduces the hardness and modulus of elasticity. As can be seen from Figure 3, the amount of free α-Ti (light areas) increases with decreasing aluminum molar fraction. To increase the content of intermetallic phases in the material, it is necessary to use compositions with a lower molar amount of titanium, and the synthesized materials must be subjected to heat treatment, the regime parameters of which will need to be further studied. The mechanical properties of pure γ-TiAl intermetallic compound at room temperature strongly depend on the purity and impurities, the type and parameters of the microstructure, and the grain size.

Therefore, the mechanical properties of the γ-TiAl intermetallic compound vary over a wide range [55–60]. For example, the compressive strength is 350–580 MPa, and the relative deformation is 0.5–1.5%. However, the elastic modulus depends, to a lesser extent, on the above factors and is equal to 175 GPa. The obtained materials of compositions I and II due to the formation of additional intermetallic phases (mainly due to Ti_3Al) have higher elastic modulus values than pure γ-TiAl intermetallic compounds. However, for composition III, the elastic modulus is at this level or slightly lower, which indicates the influence of free α-Ti in the material (the elastic modulus of titanium is 100 GPa). It can be noted that an increased α-Ti content in the material of composition III will increase its relative tensile strain at low temperatures.

Table 3. Mechanical and tribological properties.

Parameter	Composition		
	I	II	III
Hardness, GPa	9.4–10.2	8.7–9.1	6.8–8.1
Modulus of elasticity, GPa	187–215	177–185	151–170
Wear, $10^{-4} \times mm^3/N/m$	1.03	4.07	4.64
Friction coefficient	0.1	0.25	0.22

It should be noted that the obtained intermetallic composites have a Young's moduli that is similar or higher than the Young's moduli for known intermetallic materials based on titanium aluminides alloyed with the chemical elements V, Mo, Nb, Zr, etc., and obtained in the cast state [58]. Particularly distinguished is composition *I*, in which the modulus of elasticity reaches up to 215 GPa. In this work, TiAl-based intermetallic materials were obtained without the use of expensive chemical elements, such as niobium and vanadium, which significantly reduces their manufacturing cost.

3.4. Tribological Characteristics

For all samples, sliding was accompanied by sticking wear products on the Al_2O_3 ceramic counterbody. Figure 4 shows that the composition of intermetallic materials significantly affects the friction coefficient, which varies from 0.1 to 0.25. It has been established that, for all compositions, the area of the counterbody running onto the surface of the studied materials is practically the same value (the counterbody run length was about 8 m, Figure 4), after which the friction coefficient stabilizes. In this case, the friction coefficient for composition I for the first 8 m of run almost immediately has a value of 0.2, which subsequently decreases to 0.1 and then does not change with time. For compositions II and III, the friction coefficient values at the initial stage have an increasing effect, which stabilizes at values of 0.25 and 0.22 after 8 m of run, respectively (Table 3).

It should also be noted that, for composition II, the friction coefficient is somewhat higher than that of composition III, which can be explained by their different quantitative phase compositions. The reduced friction coefficient for composition I can be explained by the presence of a softer $TiAl_3$ matrix in the intermetalide material, which, during friction, acts as a lubricant between the intermetallic compound and the counterbody. It has been established that, for the material of composition *I*, wear is 4–4.5 times lower than for other compositions. In Figure 4, one can observe a smaller depth and width of the wear groove. In this case, the reduced wear value of the sample of composition *I* can be explained by its higher hardness compared to the samples of compositions II and III, as well as the presence of a softer $TiAl_3$ matrix, which acts as a friction damper. Composition *I* contains a softer $TiAl_3$ phase compared to the TiAl and Ti_3Al phases. During friction, due to the increase in temperature, the $TiAl_3$ phase becomes more plastic and acts as a lubricant in the tribocontact between the substrate and the indenter. Due to this, the coefficient of friction decreases. There is no $TiAl_3$ in the compositions of the II and III phases, meaning

that friction coefficient increased by more than four times. This confirms the assumption regarding the influence of the $TiAl_3$ phase on the friction coefficient.

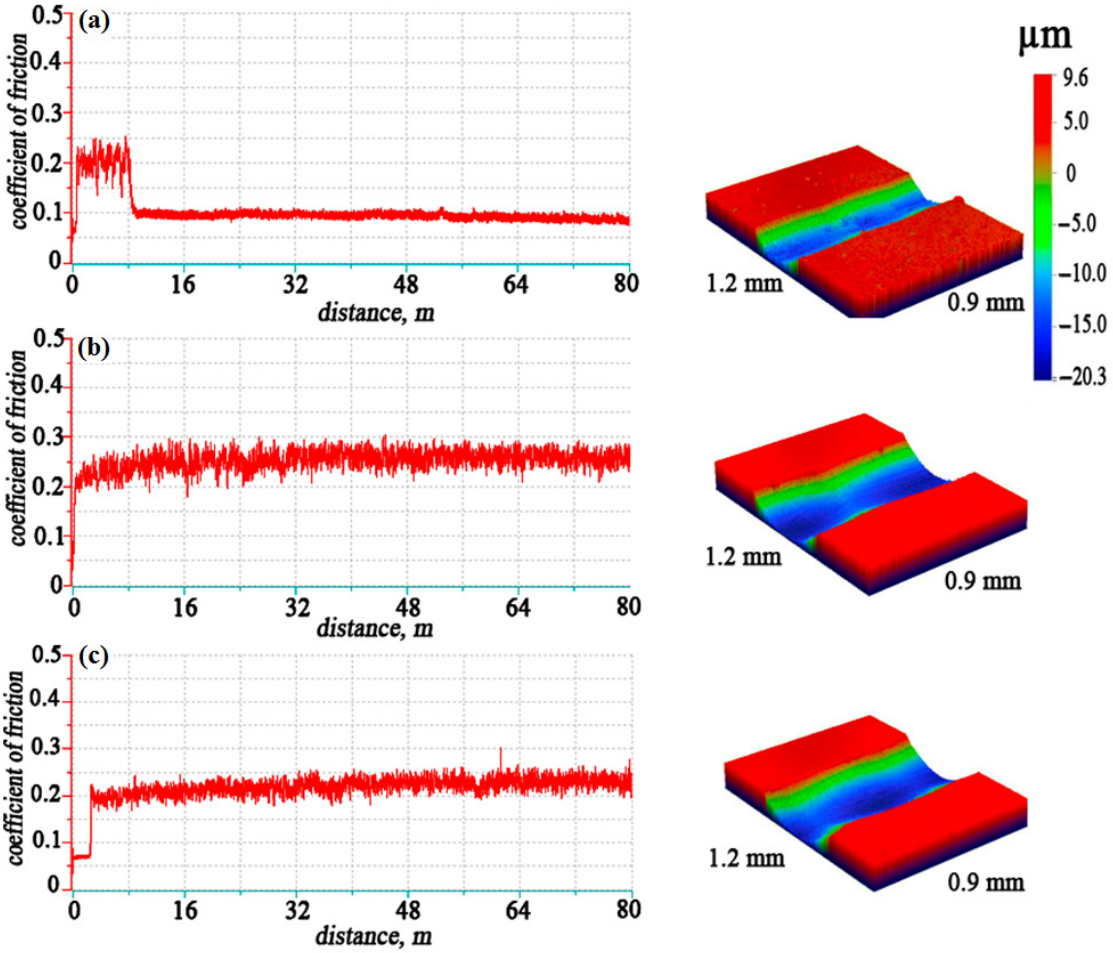


Figure 4. Dependences of the friction coefficient on the length of the run of the counterbody and the 3D profile of the wear groove for the composition materials: (**a**) I, (**b**) II, and (**c**) III.

4. Conclusions

(1) Under the conditions of free SHS compression, from the initial components of titanium and aluminum, intermetallic materials based on γ-TiAl were obtained and in situ strengthened by the Ti_3Al phase. To increase the exothermicity of the studied compositions, a chemical furnace based on the Ti–C composition was used, which made it possible to increase the combustion temperature and stabilize the combustion front. It is shown that by changing the composition and synthesis time, it is possible to control the phase composition and structure of the material.

(2) It has been established that a decrease in the molar fraction of titanium and an increase in the molar fraction of aluminum in the initial mixture leads to an increase in the mechanical and tribological characteristics of intermetallic materials, as well as their mechanical and tribological properties.

(3) It has been established that, for the material of the initial composition Ti–Al, the wear is 4–4.5 times lower and the friction coefficient is 2.4 times lower as compared to the compositions 1.5 Ti–Al and 3 Ti–Al in the Al_2O_3 intermetallic–ceramic friction pair. In this case, the size of the running-in area of the Al_2O_3 ceramic counterbody to the surface of the studied materials has practically the same value.

Author Contributions: V.A.: Writing—Review & Editing; A.B.: Formal analysis, Visualization; M.A.: Investigation, Formal analysis; A.S.: Investigation, Formal analysis, Visualization; P.B.: Conceptualization, Methodology; writing—original draft preparation. All authors have read and agreed to the published version of the manuscript.

Funding: This work was supported by the Ministry of Science and Higher Education of the Russian Federation as part of the State Assignment of the Merzhanov Institute of Structural Macrokinetics and Materials Sciences of the Russian Academy of Sciences (ISMAN) and the State Assignment of the Kurnakov Institute of General and Inorganic Chemistry of the Russian Academy of Sciences (IGIC RAS). The work was carried out using the equipment of the Distribution Center for Collective Use of the Merzhanov Institute (ISMAN). The authors thank the Ministry of Science and Higher Education of the Russian Federation.

Conflicts of Interest: The authors declare that they have no conflict of interest.

References

1. Bewlay, B.P.; Nag, S.; Suzuki, A.; Weimer, M.J. TiAl alloys in commercial aircraft engines. *Mater. High Temp.* **2016**, *33*, 549–559. [CrossRef]
2. Clemens, H.; Mayer, S. Intermetallic titanium aluminides in aerospace applications—Processing, microstructure and properties. *Mater. High Temp.* **2016**, *33*, 560–570. [CrossRef]
3. Yang, K.; Shi, X.; Zhai, W.; Chen, L.; Zhang, A.; Zhang, Q. Tribological behavior of TiAl matrix self-lubricating composites reinforced by multilayer grapheme. *RSC Adv.* **2015**, *5*, 44618–44625. [CrossRef]
4. Xu, Z.; Yao, J.; Shi, X.; Shi, X.; Zhai, W.; Ibrahim, A.M.M.; Xiao, Y.; Chen, L.; Zhu, Q.; Zhang, A. A study of the frictional layer of TiAl-12Ag-5TiB_2 composite during dry sliding wear. *J. Mater. Eng. Perform.* **2015**, *24*, 2875–2884. [CrossRef]
5. Kang, Y.; Hongru, M.; Xiyao, L.; Yangming, Z. Effect of the micro-structure evolution of friction layer on the sliding tribology behavior of TiAl-10 wt.% Ag at 16 N-0.5 m/s. *Ind. Lubr. Tribol.* **2018**, *70*, 1676–1683. [CrossRef]
6. Yang, K.; Shi, X.; Huang, Y.; Liu, X.; Wang, Y. A study of the friction layer of TiAl-10 wt.% Ag composite and the prediction model of friction and wear behaviors. *Proc. Inst. Mech. Eng. J. J. Eng. Tribol.* **2018**, *232*, 699–710. [CrossRef]
7. Yu, S.; Zhan, X.; Liu, F.; Guo, Y.; Wang, Q.; Li, Y.; Wang, Z.; Wang, Z.; Tan, L.; Fan, X.; et al. 900 °C oxidation resistance of Ni-base superalloys alloyed with different refractory elements. *J. Alloys Compd.* **2022**, *904*, 164071. [CrossRef]
8. Hagen, S.P.; Weiser, M.; Abu-Khousa, B.; Virtanen, S. Influence of the Co/Ni ratio and dendritic segregations on the high-temperature oxidation resistance of multinary Co-rich superalloys at 850 °C and 1050 °C. *Metall. Mater. Trans. A Phys. Metall. Mater. Sci.* **2022**, *53*, 1552–1571. [CrossRef]
9. Dhinakaran, V.; Ajith, J.; Fathima Yasin Fahmidha, A.; Jagadeesha, T.; Sathish, T.; Stalin, B. Wire arc additive manufacturing (WAAM) process of nickel based superalloys—A review. *Mater. Today Proc.* **2020**, *21*, 920–925. [CrossRef]
10. Xu, R.; Li, M.; Zhao, Y. A review of microstructure control and mechanical performance optimization of γ-TiAl alloys. *J. Alloys Compd.* **2023**, *932*, 167611. [CrossRef]
11. Ye, X.C.; Xiao, K.Q.; Cao, R.X.; Wu, H.; Zhao, G.; Li, B. Microstructure evolution and microhardness of TiAl based alloy blade by vacuum suction casting. *Vacuum* **2019**, *163*, 186–193. [CrossRef]
12. Narayana, P.L.; Kim, J.H.; Yun, D.W.; Kim, S.E.; Reddy, N.S.; Yeom, J.T.; Seo, D.; Hong, J.K. High temperature isothermal oxidation behavior of electron beam melted multi-phase γ-TiAl alloy. *Intermetallics* **2022**, *141*, 107424. [CrossRef]
13. Lu, X.; Li, J.; Chen, X.; Qiu, J.; Wang, Y.; Liu, B.; Liu, Y.; Rashad, M.; Pan, F. Mechanical, tribological and electrochemical corrosion properties of in-situ synthesized Al_2O_3/TiAl composites. *Intermetallics* **2020**, *120*, 106758. [CrossRef]
14. Wang, H.; Wang, Q.; Zeng, L.; Zhang, H.; Ding, H. Microstructure, mechanical and tribological performances of a directionally solidified γ-TiAl alloy. *Mater. Charact.* **2021**, *179*, 111393. [CrossRef]
15. Zhang, N.; Sun, D.; Han, X.; Wang, D.; Wang, Q.; Liu, H.; Yu, Z. Dry-sliding tribological properties of TiAl alloys and Ti_2AlN/TiAl composites at high temperature. *J. Mater. Eng. Perform.* **2018**, *27*, 6107–6117. [CrossRef]
16. Yanga, K.; Shi, X.; Huang, Y.; Wang, Z.; Wang, Y.; Zhang, A.; Zhang, Q. The research on the sliding friction and wear behaviors of TiAl-10 wt.% Ag at elevated temperatures. *Mater. Chem. Phys.* **2017**, *186*, 317–326. [CrossRef]
17. Wei, D.B.; Zhou, X.; Li, F.K.; Li, M.F.; Li, S.Q.; Zhang, P.Z. Effects of plasma surface Ta alloying on the tribology behavior of γ-TiAl. *J. Min. Metall. B* **2021**, *57*, 97–104. [CrossRef]
18. Mengis, L.; Grimme, C.; Galetz, M.C. Tribological properties of the uncoated and aluminized Ti–48Al–2Cr–2Nb TiAl alloy at high temperatures. *Wear* **2021**, *477*, 203818. [CrossRef]
19. Yang, K.; Ma, H.; Li, X.; He, Q. The analysis in in situ preparation, mechanics, and tribology of TiAl–SnAgCu/Graphene composites. *Adv. Eng. Mater.* **2018**, *20*, 1800719. [CrossRef]
20. Shen, Q.; Shi, X.; Yang, K.; Zou, J.; Zhai, W.; Huang, Y. Tribological performance of TiAl matrix composites containing silver and V_2O_5 nanowires at elevated temperatures. *RSC Adv.* **2016**, *61*, 56294–56302. [CrossRef]
21. Ozge, G.; Rahmi, U. Development of gamma titanium aluminide (γ-TiAl) alloys: A review. *J. Alloys Compd.* **2022**, *929*, 167262. [CrossRef]

22. Laska, N.; Bauer, P.P.; Helle, O.; Kreps, F. Sputtering and characterization of MAX-phase forming Cr–Al–C and Ti–Al–C coatings and their application on γ-based titanium aluminides. *Adv. Eng. Mater.* **2022**, *24*, 2100722. [CrossRef]
23. Mengis, L.; Grimme, C.; Galetz, M.C. High-temperature sliding wear behavior of an intermetallic γ–based TiAl Alloy. *Wear* **2018**, *426–427*, 341–347. [CrossRef]
24. Li, D.; Wang, B.; Luo, L.; Li, X.; Yu, J.; Wang, L.; Xu, Y.; Su, Y.; Guo, J.; Fu, H. In-situ synthesis of Al_2O_3-reinforced high Nb–TiAl laminated composite with an enhanced strength-toughness performance. *Ceram. Int.* **2022**, *48*, 1589–1602. [CrossRef]
25. Li, J.; Hu, R.; Zhou, M.; Gao, Z.; Wu, Y.; Luo, X. High temperature micromechanical behavior of Ti_2AlN particle reinforced TiAl based composites investigated by in-situ high-energy X-ray diffraction. *Mater. Des.* **2021**, *212*, 110225. [CrossRef]
26. Shen, J.; Hu, L.; Zhang, L.; Liu, W.; Fang, A.; Sun, Y. Synthesis of TiAl/Nb composites with concurrently enhanced strength and plasticity by powder metallurgy. *Mater. Sci. Eng. A* **2020**, *795*, 139997. [CrossRef]
27. Jie, L.; Tongli, W.; Mengfei, W.; Li, W.; Qi, Z.; Kehong, W.; Peter, S.; Norbert, S.; Norbert, H.; Nikolai, K. In situ observation of competitive growth of α grains during β → α transformation in laser beam manufactured TiAl alloys. *Mater. Charact.* **2021**, *179*, 111371. [CrossRef]
28. Ren, H.S.; Shang, Y.L.; Ren, X.Y.; Jing, Y.J.; Xiong, H.P.; Cheng, Y.Y. Microstructure and mechanical properties of TiAl/TiAl joints brazed with a newly developed Ti–Ni–Nb–Zr quaternary filler alloy. *Prog. Nat. Sci. Mater. Int.* **2022**, *32*, 758–768. [CrossRef]
29. Ye, L.H.; Hao, W.; Gang, Z.; Hu, Q.M.; Rui, Y. Phase stability of TiAl-X (X=V, Nb, Ta, Cr, Mo, W, and Mn) alloys. *J. Alloys Compd.* **2020**, *819*, 153291. [CrossRef]
30. Xiao, S.L.; Xu, L.J.; Yu, H.B.; Tian, J.; Chen, Y.Y. Microstructure and mechanical properties of Ti–45Al–5.5(Cr,Nb,B,Ta) alloy sintered at different SPS temperatures. *Trans. Nonferrous Met. Soc. China* **2012**, *22*, 2960–2964. [CrossRef]
31. Lapin, J. Creep behavior of a cast intermetallic Ti–45.2Al–2W–0.6Si–0.7B alloy. *Scr. Mater.* **2004**, *50*, 261–265. [CrossRef]
32. Dong, S.; Qu, Y.; Chen, R.; Li, G.; Zhang, W.; Wang, Q.; Fang, H.; Guo, J. Proper (Nb,Fe) co-alloyed TiAl-based alloy with good hot deformation processing capability. *Intermetallics* **2023**, *153*, 107780. [CrossRef]
33. Li, M.; Li, J.; Zhou, T.; Hu, L.; Shi, L.; Chen, Y.; Xu, L. Microstructure evolution, deformation behavior and manufacture design of TiAl matrix composites reinforced with in-situ borides precipitation. rans. *Nonferrous Met. Soc. China* **2023**, *33*, 107–127. [CrossRef]
34. Liang, X.; Liu, Z.; Li, H.; Chen, F.; Yang, W.; Ouyang, S.; Liu, Y.; Wang, L. Microstructure and elevated-temperature mechanical properties of in situ Ti2AlNb-reinforced TiAl-matrix composite prepared by powder metallurgy. *Mater. Today Commun.* **2020**, *24*, 101179. [CrossRef]
35. Noda, T.; Okabe, M.; Isobe, S.; Sayashi, M. Silicide precipitation strengthened TiAl. *Mater. Sci. Eng. A* **1995**, *192–193*, 774–779. [CrossRef]
36. Li, P.; Yang, Y.Q.; Koval, V.; Chen, J.; Luo, X.; Zhang, W.; Wang, B. Temperature-dependent deformation processes in two-phase TiAl + Ti3Al nano-polycrystalline alloys. *Mater. Des.* **2021**, *199*, 109422. [CrossRef]
37. Bazhina, A.D.; Konstantinov, A.S.; Chizhikov, A.P.; Avdeeva, V.V.; Bazhin, P.M. Materials based on the MAX phases of the Ti-Al-C system obtained under combustion and high-temperature shear deformation. *Mater. Lett.* **2022**, *318*, 132196. [CrossRef]
38. Bazhin, P.M.; Stolin, A.M.; Konstantinov, A.S.; Chizhikov, A.P.; Prokopets, A.D.; Alymov, M.I. Structural features of titanium boride-based layered composite materials produced by free SHS compression. *Dokl. Chem.* **2019**, *488*, 246–248. [CrossRef]
39. Bazhina, A.; Chizhikov, A.; Konstantinov, A.; Khomenko, N.; Bazhin, P.; Avdeeva, V.; Chernogorova, O.; Drozdova, E. Structure, phase composition and mechanical characteristics of layered composite materials based on TiB/xTi-Al/α-Ti (x = 1, 1.5, 3) obtained by combustion and high-temperature shear deformation. *Mater. Sci. Eng. A* **2022**, *858*, 144161. [CrossRef]
40. Bazhina, A.; Konstantinov, A.; Chizhikov, A.; Bazhin, P.; Stolin, A.; Avdeeva, V. Structure and mechanical characteristics of a layered composite material based on TiB/TiAl/Ti. *Ceram. Int.* **2022**, *48*, 14295–14300. [CrossRef]
41. Prokopets, A.D.; Bazhin, P.M.; Konstantinov, A.S.; Antipov, M.S.; Avdeeva, V.V. Structural features of layered composite material $TiB_2/TiAl/Ti_6Al_4$ obtained by unrestricted SHS-compression. *Mater. Lett.* **2021**, *300*, 130165. [CrossRef]
42. Tomilin, O.B.; Muryumin, E.E.; Fadin, M.V.; Shchipakin, S.Y. Preparation of luminophore $CATIO_3:PR^{3+}$ by self-propagating high-temperature synthesis. *Russ. J. Inorg. Chem.* **2022**, *67*, 431–438. [CrossRef]
43. Levashov, E.A.; Mukasyan, A.S.; Rogachev, A.S.; Shtansky, D.V. Self-propagating high-temperature synthesis of advanced materials and coatings. *Int. Mater. Rev.* **2017**, *62*, 203–239. [CrossRef]
44. Radishevskaya, N.I.; Nazarova, A.Y.; L'vov, O.V.; Kasatskii, N.G.; Salamatov, V.G.; Saikov, I.V.; Kovalev, D.Y. Self-propagating high-temperature synthesis of $MgAl_2O_4$ spinel. *Inorg. Mater.* **2020**, *56*, 142–150. [CrossRef]
45. Li, C.X.; Xia, J.; Dong, H. Sliding wear of TiAl intermetallics against steel and ceramics of Al_2O_3, Si_3N_4 and WC/Co. *Wear* **2006**, *261*, 693–701. [CrossRef]
46. Levashov, E.A.; Shtansky, D.V.; Kiryukhantsev-Korneev, P.V.; Petrzhik, M.I.; Tyurina, M.Y.; Sheveiko, A.N. Multifunctional nanostructured coatings: Formation, structure, and the uniformity of measuring their mechanical and tribological properties. *Russ. Metall.* **2010**, *10*, 917–935. [CrossRef]
47. Rogachev, A.S. Mechanical activation of heterogeneous exothermic reactions in powder mixtures. *Russ. Chem. Rev.* **2019**, *88*, 875–900. [CrossRef]
48. Dreizin, E.L.; Schoenitz, M. Mechanochemically prepared reactive and energetic materials: A review. *J. Mater. Sci.* **2017**, *52*, 11789–11809. [CrossRef]
49. Lapshin, O.V.; Boldyreva, E.V.; Boldyrev, V.V. Role of mixing and milling in mechanochemical synthesis (review). *Russ. J. Inorg. Chem.* **2021**, *66*, 433–453. [CrossRef]

50. Kim, J.Y.; Park, E.S.; Lee, T.; Ryu, S.; Kim, S.E.; Kim, S.W. Origin of enhanced room temperature ductility in TiAl alloys: Reducing activation difference of deformation mechanism of γ phase. *J. Alloys Compd.* **2022**, *899*, 163307. [CrossRef]
51. Prokopets, A.D.; Konstantinov, A.S.; Chizhikov, A.P.; Bazhin, P.M.; Stolin, A.M. General trends of structure formation in graded composite materials based on the Ti_3AlC_2 MAX Phase on titanium. *Inorg. Mater.* **2020**, *56*, 1087–1091. [CrossRef]
52. Stolin, A.M.; Bazhin, P.M.; Konstantinov, A.S.; Alymov, M.I. Production of large compact plates from ceramic powder materials by free SHS compaction. *Dokl. Chem.* **2018**, *480*, 136–138. [CrossRef]
53. Bazhin, P.; Konstantinov, A.; Chizhikov, A.; Prokopets, A.; Bolotskaia, A. Structure, physical and mechanical properties of TiB-40 wt.% Ti composite materials obtained by unrestricted SHS compression. *Mater. Today Commun.* **2020**, *25*, 101484. [CrossRef]
54. Antipov, M.S.; Bazhin, P.M.; Chizhikov, A.P.; Konstantinov, A.S.; Stolin, A.M.; Khomenko, N.Y. Formability, phase composition, and microstructure of TiC–(5–50 wt%) NiCr–based materials obtained by free SHS compression. *Russ. J. Inorg. Chem.* **2022**, *67*, 1658–1664. [CrossRef]
55. Bazhina, A.D.; Bazhin, P.M.; Chizhikov, A.P.; Konstantinov, A.S.; Stolin, A.M. Influence of high-temperature annealing on structure of titanium aluminide materials obtained by combustion and high-temperature shear deformation. *Intermetallics* **2021**, *139*, 107313. [CrossRef]
56. Duan, B.; Yang, Y.; He, S.; Feng, Q.; Mao, L.; Zhang, X.; Jiao, L.; Lu, X.; Chen, G.; Li, C. History and development of γ-TiAl alloys and the effect of alloying elements on their phase transformations. *J. Alloys Compd.* **2022**, *909*, 164811. [CrossRef]
57. Güther, V.; Allen, M.; Klose, J.; Clemens, H. Metallurgical processing of titanium aluminides on industrial scale. *Intermetallics* **2018**, *103*, 12–22. [CrossRef]
58. Wimler, D.; Lindemann, J.; Kremmer, T.; Clemens, H.; Mayer, S. Microstructure and mechanical properties of novel TiAl alloys tailored via phase and precipitate morphology. *Intermetallics* **2021**, *138*, 107316. [CrossRef]
59. Imayev, V.M.; Ganeev, A.A.; Trofimov, D.M.; Parkhimovich, N.J.; Imayev, R.M. Effect of Nb, Zr and Zr + Hf on the microstructure and mechanical properties of β-solidifying γ-TiAl alloys. *Mater. Sci. Eng. A* **2021**, *817*, 141388. [CrossRef]
60. Vardanyan, E.L.; Ramazanov, K.N.; Nagimov, R.S.; Nazarov, A.Y. Properties of intermetallic Ti-Al based coatings deposited on ultrafine grained martensitic steel. *Surf. Coat. Technol.* **2020**, *389*, 125657. [CrossRef]

Disclaimer/Publisher's Note: The statements, opinions and data contained in all publications are solely those of the individual author(s) and contributor(s) and not of MDPI and/or the editor(s). MDPI and/or the editor(s) disclaim responsibility for any injury to people or property resulting from any ideas, methods, instructions or products referred to in the content.